A Survey of Self-Interference in LTE-Advanced and 5G New Radio Wireless Transceivers

Silvester Sadjina, *Student Member, IEEE*, Christian Motz, *Student Member, IEEE*, Thomas Paireder, *Student Member, IEEE*, Mario Huemer, *Senior Member, IEEE*, and Harald Pretl, *Senior Member, IEEE*

***Abstract*— This article presents a comprehensive survey of the literature on self-interference (SI) in long-term evolution advanced (LTE-A) and fifth-generation (5G) new radio transceivers and should serve the reader as a guide and starting point for further work on SI management. Current trends in cellular transceiver designs are discussed, and reasons why new technologies, such as carrier aggregation, cause potential sensitivity degradation due to self-interfering signals are highlighted. The survey provides an overview of the most common interference mechanisms and continues with a taxonomy on SI mitigation architectures by comparing the strengths and weaknesses of various techniques.**

***Index Terms*— Carrier aggregation (CA), cellular hand-set, fifth generation (5G), frequency division duplex (FDD), interference cancellation, long-term evolution advanced (LTE-A), self-interference (SI).**

I. Introduction

CELLULAR networks evolve constantly to meet the demand in increasing data transmission rates. New technologies, such as long-term evolution advanced (LTE-A) or fifth-generation (5G) new radio (NR), introduce new techniques, such as carrier aggregation (CA), high-order modulation (HOM), and multiple-input and multiple-output (MIMO) techniques, to attain peak data rates up to several Gb/s. The user equipment (UE) requires a small form factor and low power consumption of the radio frequency (RF) transceiver, making single-chip RF designs—covering NR and legacy protocols simultaneously—essential. The integration on a single chip and the increasing complexity of transceivers cause potential receive (RX) sensitivity degradation due to interfering signals.

Manuscript received July 4, 2019; revised September 29, 2019; accepted October 9, 2019. Date of publication February 20, 2020; date of current version March 4, 2020. This work was supported in part by the Austrian Federal Ministry for Digital and Economic Affairs and in part by the National Foundation for Research, Technology and Development. *(Corresponding author: Silvester Sadjina.)*

S. Sadjina, C. Motz, and T. Paireder are with Intel DMCE, 4040 Linz, Austria, and also with the Christian Doppler Laboratory for Digitally Assisted RF Transceivers for Future Mobile Communications, Johannes Kepler University, 4040 Linz, Austria (e-mail: silvester.sadjina@intel.com).

M. Huemer is with the Christian Doppler Laboratory for Digitally Assisted RF Transceivers for Future Mobile Communications, Johannes Kepler University, 4040 Linz, Austria.

H. Pretl is with Intel DMCE, 4040 Linz, Austria, and also with the Institute for Integrated Circuits, Johannes Kepler University, 4040 Linz, Austria.

Color versions of one or more of the figures in this article are available online at http://ieeexplore.ieee.org.

Digital Object Identifier 10.1109/TMTT.2019.2951166

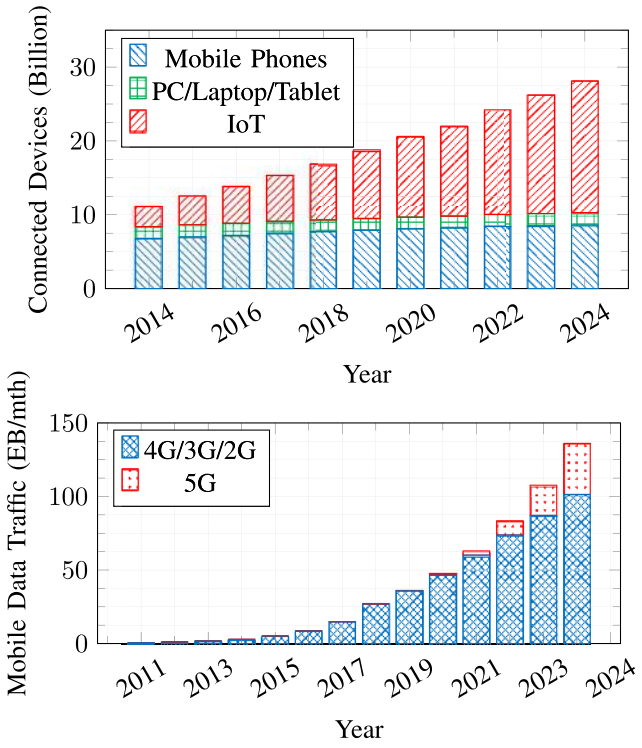

Fig. 1. Need for speed and capacity [1] in LTE-A and 5G NR transceivers. New technologies, such as HOM, CA, or MIMO, are required to meet the demand in increasing data transmission rates.

Compared with other interfering signals as specified in the third-generation partnership project (3GPP) standards, self-interference (SI) can result in the most severe performance degradation of the receiver. Due to the implementation of new techniques such as CA and due to the increasing number of operating frequencies and band combinations, relying solely on passive interference mitigation might not be sufficient for the state-of-the-art transceivers. To mitigate the self-interfering signals, the employment of active techniques in the analog or digital domain is beneficial, which increases the suppression in addition to the passive filtering. The high complexity and nonlinear behavior of RF front ends (FEs) result in a multitude of SI mechanisms that cannot be targeted with traditional approaches. Receiver desense by intermodulation (IM) or harmonics of SI signals have to be targeted with advanced mitigation architectures, which allow the receiver to sustain the required sensitivity in such scenarios [2].

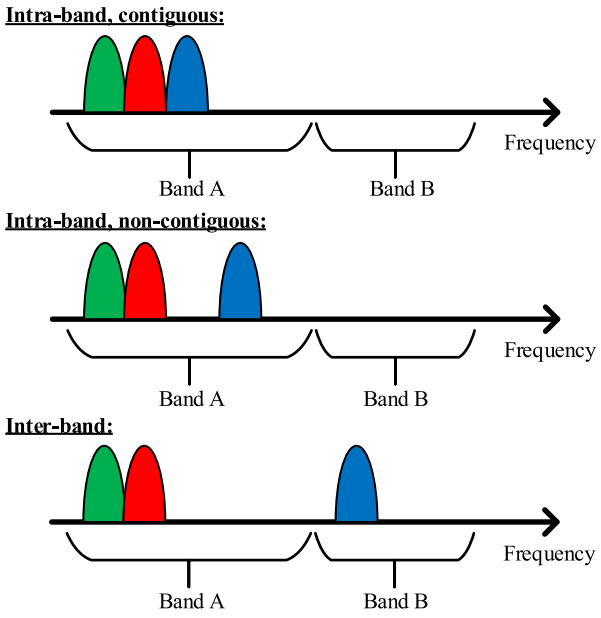

Fig. 2. Types of CA. In LTE-A and 5G NR transceivers, multiple component carriers can be aggregated to increase the total BW.

This article provides a comprehensive overview on SI in LTE-A and 5G NR CA transceivers. Further surveys and tutorials on SI can be found in [3]–[7]. Section II describes current trends in RF FEs and highlights why interference scenarios are increasing. Prevailing interference mechanisms are categorized in Section III followed by an overview in Section IV on the most common interference mitigation techniques.

II. Trends in RF Front-Ends

Worldwide mobile broadband subscriptions and data traffic per smartphone are increasing drastically, as shown in Fig. 1. This growing demand can only be met with the introduction of new concepts and architectures for mobile transceivers [1]. The upgrade of long-term evolution (LTE) from the basic data rate of 150 Mb/s toward several Gb/s required the introduction of different techniques, such as using HOM of up to 256 quadrature amplitude modulation (QAM) and 1024 QAM, respectively, stepping up MIMO to 4×4 configurations and the aggregation of several channels (each up to 400 MHz wide) to increase the total transmission bandwidth (BW) [8], [9]. Furthermore, high-power user equipment (HPUE) extends the range and uplink (UL) throughput.

The technique to increase the total bandwidth (BW) by channel bonding is called CA. The three basic aggregation scenarios are: 1) intraband contiguous (Intra-C); 2) intraband noncontiguous (Intra-NC); and 3) interband (Inter), which are shown in Fig. 2 for a three-CA scenario. The carriers are named the primary component carrier (PCC) and the secondary component carrier (SCC), respectively. In the frequency division duplex (FDD) operation, the transmit (TX) signal is located at the duplex distance of the PCC. While intraband contiguous CA is mostly implemented using a single RX path with extended BW of $n \cdot \mathrm{BW_{RX}}$ MHz, the noncontiguous case and the interband aggregation use a multitude

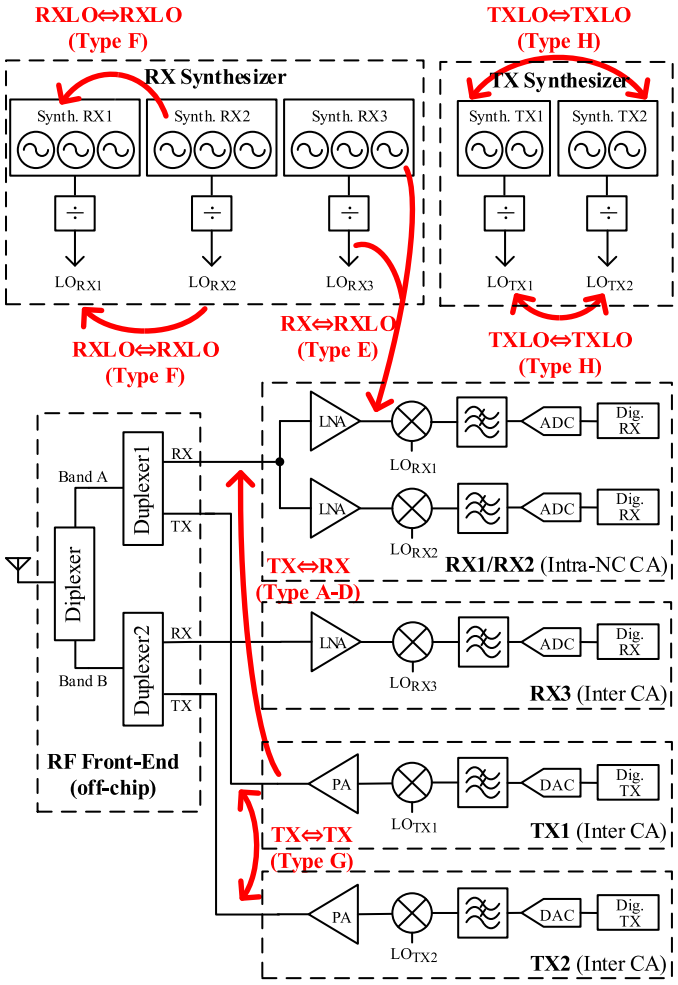

Fig. 3. Coupling mechanism categorized causing SI.

of RX chains and phase-locked loops (PLLs) to receive the wanted channels [2]. The 3GPP standard now supports CA of up to five bands in downlink [8]. In combination with interband CA in UL, a large number of local oscillators (LO) and RF signals have to be managed inside a wireless transceiver IC (exemplary shown in Fig. 3), necessitating the use of interference, cross-talk prevention techniques (CPT), and cancellation technique. Therefore, CA is the primary driver of an ever-increasing number of interference scenarios appearing in the state-of-the-art transceivers. In addition to CA in LTE-A, the introduction of 5G NR will happen in nonstandalone configuration first, i.e., a handset in dual-connectivity is simultaneously connected to an LTE-A as well as a 5G NR network, a situation quite similar to CA, but with increased complications due to different timings [10]. Also, the usage of HPUE introduces more stringent linearity requirements for transmitter design.

To support a variety of different CA scenarios and LTE band combinations, new architectures are required: Table I gives an overview over different receiver CA implementations. Most of the published works use an architecture where an incoming RF signal is received by N low-noise amplifier input ports and directly downconverted by M RF chains [mixer, LO, baseband (BB)] per component carrier using RF routing.

TABLE I
RX CA IMPLEMENTATIONS

Type	Implementation	Publications
Inter	One RX per band (Intra-C or Intra-NC capable)	[2], [12]–[14], [15]–[19]
Intra-C	Implementation by wide RX BW	[20], [21]
Intra-NC	Split-by-N LNA and use M-multiple RX (mixer, LO, BB) per CC using RF routing	[2], [13], [14], [22], [17], [23], [24], [16], [18]
	Split-by-N LNA and use M-multiple RX (mixer, LO, BB) per CC using LO routing	[15]
	Analog double-conversion using low IF	[12]
	Analog double-conversion using high IF	[11], [22], [25]
	Analog/digital double-conversion using single RX and digital second conversion	[26]

With this type of CA implementation, a multitude of different RF signals is operating in the same time on the transceiver which, together with the direct-conversion architecture using multiple LO signals, results in a setup prone to interference-induced performance degradation. Other types [11] have been proposed, which are more resistant to interfering signals and crosstalk mechanisms by using double-conversion architectures.

Nevertheless, direct-conversion architectures are still preferred in commercial designs due to their superior RF performance and lower complexity [13], [14], [22].

III. SELF-INTERFERENCE MECHANISMS

This section presents an overview of different RF degradation effects for LTE-A and 5G NR CA transceivers, which are shown in Fig. 3. The shown mechanisms are categorized in Table II, including more detailed information together with examples for better understanding. LTE-A and 5G NR transmitters use distinct RX and TX paths. Fig. 3 shows a simplified block diagram of such a multiband CA transceiver, including a simplified FE utilizing two TX and two RX paths, but neglecting further MIMO or auxiliary (AUX) RX or TX paths. For a real multiband CA transceiver, additional switches and multiplexers would be required resulting in further unwanted coupling across the functional blocks. In the following summary of different RF degradation effects, transceivers utilizing either zero- or low-IF topologies, high dynamic range analog–digital-converter (ADC)/digital–analog-converter (DAC), and extensive digital signal processing in the BB are assumed.

The finite and frequency selective isolation of the duplexer between the TX and RX paths results in different interfering components, which cause receiver desensitization [27]. As shown in Fig. 4, dependent on the frequency-selective isolation of the leakage channel and dependent on the duplexing distance, different mechanisms can be dominant.

IM distortions are produced by interfering signals passing through nonlinear components in the RX path (Type A). In direct-conversion receivers, even-order IM products degrade the performance of the receiver. Second-order IM distortions are most severe, but especially in cell-edge scenarios with high TX power level, also higher orders can be dominant.

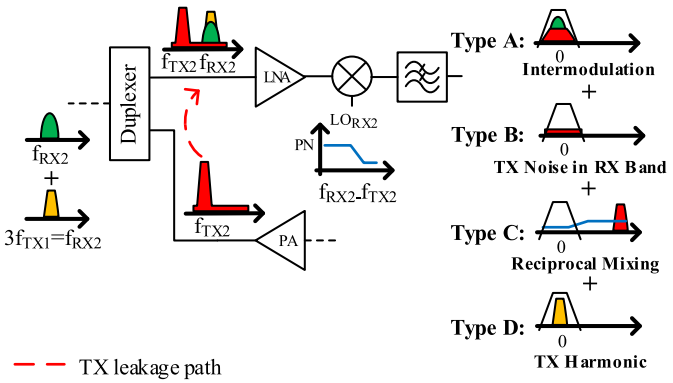

Fig. 4. Receiver desensitization in the presence of strong TX leakage signal (Types A–D).

This type of interference drives the input-referred second-order intercept point (IIP2) of receivers, which is a typical bottleneck in many RF transceivers. Odd-order IM products are generated in the RF domain of the RX path and may fall at the frequency of the desired signal. The third-order IM term is most severe and defined by the full-duplex and half-duplex linearity requirements [28].

Another source of interference stems from the nonlinearity of the transmitter. The TX nonlinearities cause spectral regrowth of the modulated TX signals, which might appear as additional receive-band noise (Type B). This is especially severe in two scenarios.

1) Due to weak isolation of the transition band of the duplexer, this out-of-band emission is directly present at the receiver input and can heavily reduce the sensitivity.
2) In CA and direct-conversion transmitter, spectral regrowth can be troublesome due to a potentially much smaller duplex distance for an SCC RX.

The TX and RX signals can be close by; therefore, the out-of-band emission can directly overlap the receive signal [29].

The phase-noise (PN) of the LO adds wideband noise in the TX upconversion process (Type C). This receive-band noise can be troublesome in CA due to the potentially much smaller duplex distance for the SCC RX.

In addition, the nonlinear behavior of the power amplifier (PA) and the TX LO harmonics generate unwanted harmonic content of the TX (Type D). These harmonics may degrade the performance of the RX when they fall in-band and on top of the desired RX signal [30]. For a transceiver operating in an interband CA scenario, the condition

$$|n_1\ f_{\mathrm{TX1}} - m_2\ f_{\mathrm{RX2}}| < \frac{\mathrm{BW_{RX2}} + \mathrm{BW_{TXH}}}{2}, \quad n_1, m_2 \in \mathbb{Z}^+ \quad (1)$$

has to be fulfilled in this case, where f_{TX1} is the primary TX carrier frequency, f_{RX2} is the secondary RX carrier frequency, n_1 is the order of the TX harmonic, m_2 is the harmonic of the secondary RX LO, $\mathrm{BW_{RX2}}$ is the secondary RX BW, and $\mathrm{BW_{TXH}}$ is the TX harmonic BW. For TX harmonics generated by the nonlinear behavior of the PA, $\mathrm{BW_{TXH}} = n_1\mathrm{BW_{TX1}}$ and for the generation by the TX LO harmonic, $\mathrm{BW_{TXH}} = \mathrm{BW_{TX1}}$, where $\mathrm{BW_{TX1}}$ is the primary TX BW.

With the introduction of CA, a multitude of LO signals are required to receive the desired signals. LO signals tend

TABLE II
SOURCES AND EFFECTS OF RF SI

Type	Coupling	Mechanism		Interference	Example	Ref.
		Root Cause of Interference	Reception Mechanism		bx = LTE band x or 5G NR nx	
A	TX⇔RX	TX1 fundamental	RX2 nonlinearity	TX_1^{n1}	Critical as $f_{SCC} < f_{PCC}$	[34]
B		TX1 band noise	LO2 fundamental mixing	TX noise		[35]
C		TX1 fundamental	Reciprocal mixing with LO2 PN	LO_2 PN		[36]
D		TX2 fundamental or harmonic	LO2 fundamental or harmonic mixing	TX_2^{n2}	$3 \times f_{TX2@b17} = 1 \times f_{RX2@b4}$	[37]
E	RX⇔RX–LO	LO1 harmonic	LO2 harmonic mixing	CW	$3 \times f_{RX2@b41} = 4 \times f_{RX1@b39}$	[2]
F	RX–LO⇔RX–LO	TX1 fundamental	LO1-LO2 harmonic mixing	TX	$3 \times f_{RX1@b2} - 2 \times f_{RX2@b2} = f_{TX1@b2}$	[38]
G	TX⇔TX	TX IM	Fundamental mixing	$TX_1^{n1}+TX_2^{n2}$	$2 \times f_{TX1@b1} - 1 \times f_{TX2@b3} = f_{RX1@b1}$	[33]
H	TX–LO⇔TX–LO	Modulated TX Spur	Fundamental mixing	TX	$4 \times f_{TX1@b8} = 2 \times f_{TX2@b3} + f_{DD2@b3}$	[19]

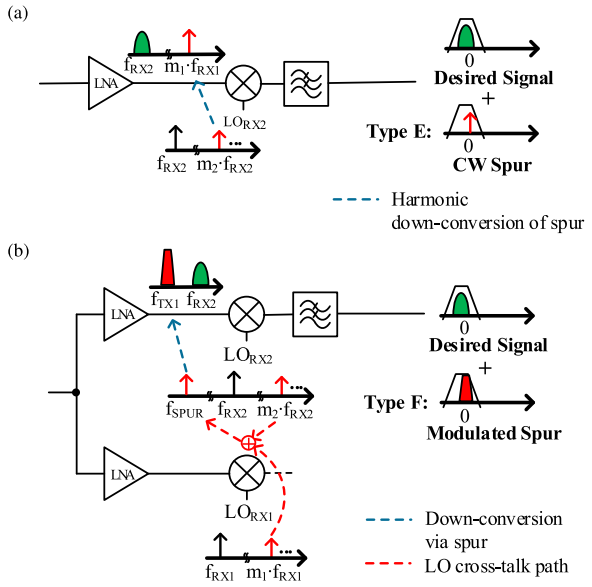

Fig. 5. Receiver desensitization due to (a) reception of alternate LO harmonic (Type E) and (b) reciprocal mixing of TX leakage signal by LO–LO spur (Type F).

to have large voltage swings, requiring only weak coupling paths for unwanted LO crosstalk. Due to these concurrently operating RF circuit blocks and due to coupling mechanism between signal traces and power supply lines, these signals may leak into the RX path, which results in spurious content being created in BB (Type E), which is shown in Fig. 5(a). In comparison to the other interference types, this mechanism can occur in FDD and time-division duplex (TDD) operations [31]. Assuming a transceiver operating in an intraband two-CA scenario, the condition

$$|m_1\ f_{RX1} - m_2\ f_{RX2}| < \frac{BW_{RX}}{2}, \quad m_1, m_2 \in \mathbb{Z}^+ \tag{2}$$

has to be fulfilled, where f_{RX1} is the primary receiver carrier frequency and m_1 is the harmonic of the primary RX LO.

With a similar mechanism, also modulated spur interference can occur in the RX chain (Type F). Fig. 5(b) shows this mechanism. Coupling between oscillators or LO distribution lines together with device nonlinearities, like nonlinearities of the LO buffers, can result in a spur which falls at the duplex distance. The modulated TX leakage signal is down-converted by this spur, subsequently becoming a modulated spur in the BB [32]. For a modulated spur to interfere with the desired signal, the condition

$$|f_{TX} - f_{SP}| < \frac{BW_{RX} + BW_{TX}}{2} \tag{3}$$

has to be fulfilled, where f_{SP} is the frequency of the LO–LO spur. Due to the coupling between LO distribution lines, the spur frequency f_{SP} is a harmonic combination of the LO signals and is given by

$$f_{SP} = |m_1\ f_{RX1} \pm m_2\ f_{RX2}|, \quad m_1, m_2 \in \mathbb{Z}^+. \tag{4}$$

When UL CA is used, the large PA output signals cause IM products (Type G), as shown in Fig. 6. Due to the nonlinear behavior of the PA, coupling in the BB can result in IM products [19]. Also, because of the nonlinearity of the FE components, TX signals passing through a common path in the FE, e.g., the antenna switch, can also result in IM products. In addition to the common path, also poor antenna isolation can result in one TX signal interfering with another one. This received signal will create IM products due to the nonlinear behavior of switches or diplexers [33]. Due to the huge difference in power between the TX and the received signals, even high-order IM products, such as IM7 or IM9, can cause unacceptable degradation of the receiver. For a transceiver operating in a dual UL CA scenario, the condition

$$|m_1\ f_{RX} - f_{IM}| < \frac{BW_{RX} + BW_{IM}}{2}, \quad m_1 \in \mathbb{Z}^+ \tag{5}$$

has to be fulfilled. The IM product frequency f_{IM} is given by

$$f_{IM} = |n_1\ f_{TX1} \pm n_2\ f_{TX2}|, \quad n_1, n_2 \in \mathbb{Z}^+ \tag{6}$$

where n_2 is the secondary TX harmonic, f_{TX2} is the secondary TX carrier frequency, and $BW_{IM} = n_1 BW_{TX1} + n_2 BW_{TX2}$ is the BW of the IM product.

TABLE III
DIFFERENT INTERFERENCE MITIGATION TECHNIQUES IN COMPARISON

Interference Mitigation Techniques	Point of Cancellation	Degree of Cancellation	Chip Area	Convergence Time	Flexibility	Reliability
Cross-talk prevention techniques (CPT)	RF+BB	**HIGH**	**HIGH**	-	**LOW**	**HIGH**
Analog interference mitigation (AIM)	RF+BB	**HIGH**	**HIGH**	MEDIUM	**LOW**	MEDIUM
Digital interference mitigation (DIM)	BB	**LOW**	**LOW**	MEDIUM	**HIGH**	**LOW**
Mixed-signal interference mitigation (MSIM)	RF+BB	MEDIUM	MEDIUM	**FAST**	MEDIUM	**HIGH**

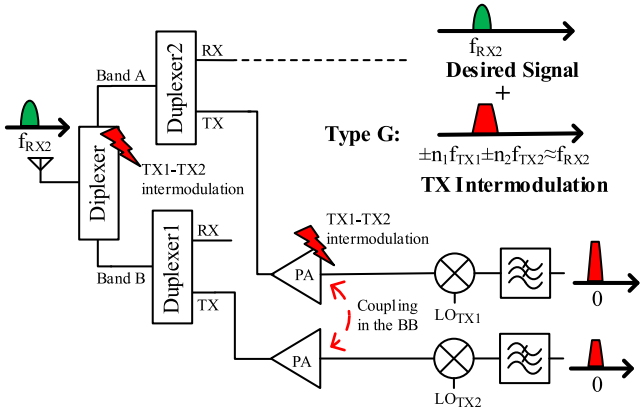

Fig. 6. Receiver desensitization by TX IM (Type G).

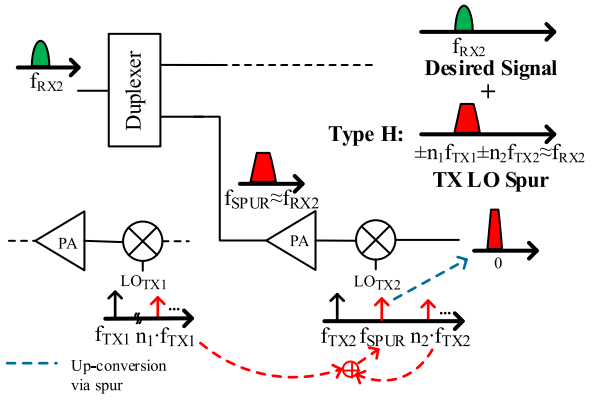

Fig. 7. Receiver desensitization by TX LO spur (Type H).

Similar to the previous effect, spurs generated due to the coupling between TX LOs or TX oscillators, falling at an RX frequency, may severely degrade the performance of the receiver (Type H). This mechanism is shown in Fig. 7. Due to the generated TX spur, the modulated TX signal is directly upconverted to the RX frequency and subsequently present in the RX chain due to the finite TX–RX isolation. This mechanism can be described with the condition

$$|m_1 \ f_{RX} - f_{SP}| < \frac{BW_{RX} + BW_{TX1}}{2}, \quad m_1 \in \mathbb{Z}^+ \tag{7}$$

with the spur frequency f_{SP} given by

$$f_{SP} = |n_1 \ f_{TX1} \pm n_2 \ f_{TX2}|, \quad n_1, n_2 \in \mathbb{Z}^+. \tag{8}$$

IV. INTERFERENCE MITIGATION TECHNIQUES

When building a wireless transceiver for LTE-A or 5G NR, the most important rule is to design the analog circuits as crosstalk resilient as possible. Thus, transceiver designs should have low emissions on one end and high interference immunity on the other end. In this section, we describe techniques for reducing crosstalk on the transceiver, followed by different interference mitigation techniques. When employing these techniques, the natural question is, whether the needed power consumption for these approaches could be used to increase the RF performance of the receiver to achieve comparable performance instead? Other factors, such as chip area and increased complexity, have also to be considered. Fig. 8 compiles a comprehensive overview about different interference mitigation techniques. In this article, these techniques are categorized into four main groups. In the first group, crosstalk prevention summarizes all techniques for reducing crosstalk and interfering signals appearing in the receiver. The other three groups target the mitigation of interference in the receiver. Here, we will differentiate between analog (second group), digital (third group), and mixed-signal (fourth group) approaches, as shown in Fig. 9. In the state-of-the-art transceivers, several techniques are combined to achieve the needed amount of interference immunity. For example, passive suppression is used to isolate the TX from the RX. The residual TX leakage is then canceled by an analog SI approach, followed by a digital cancellation architecture to further mitigate the interference [39].

Fig. 10 illustrates the increasing number of interference mitigation publications per year. Analog interference mitigation (AIM) techniques are dominant followed by CPT and digital interference mitigation (DIM) techniques. In the last years, mixed-signal interference mitigation (MSIM) also became more popular. Table III compares the different interference mitigation categories. CPT and AIM techniques provide excellent cancellation performance but suffer from high area consumption and are complex to implement. DIM techniques offer high flexibility and scalability, as the whole cancellation system is realized in pure digital. However, on the other hand, these techniques provide only a limited cancellation, especially in dynamic environments. Besides, they also suffer from having longer settling/convergence times depending on the type of interference the cancellation system is adapting. MSIM combines the flexibility of digital and reliability of analog cancellation techniques. These approaches can fastly adapt to the dynamic environment providing a reliable cancellation and are also easy to implement.

A. Cross-Talk Prevention Techniques

The best option to mitigate degradation due to interfering signals is to prevent them in the first way. In the design process of transceivers, special techniques are used to prevent crosstalk and, therefore, receiver performance degradation due to interfering signals. Different architectures, layout techniques, and

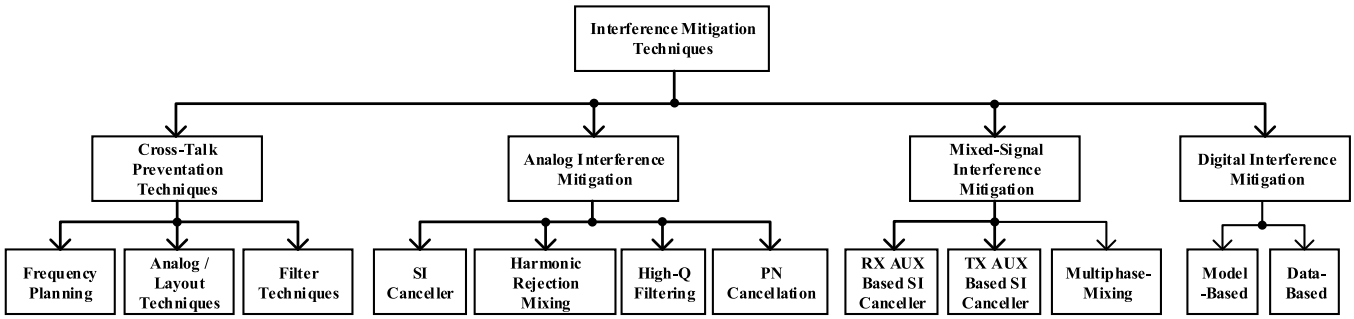

Fig. 8. Categorization of interference mitigation techniques in RF transceivers.

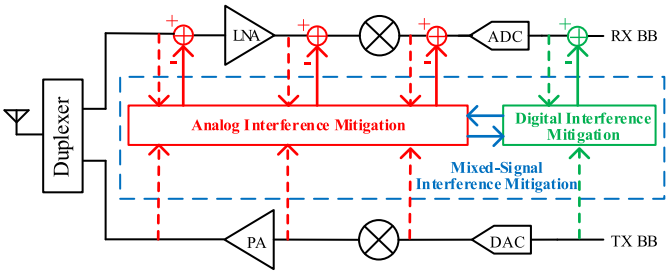

Fig. 9. Categorization of SI cancellation methods in FDD systems.

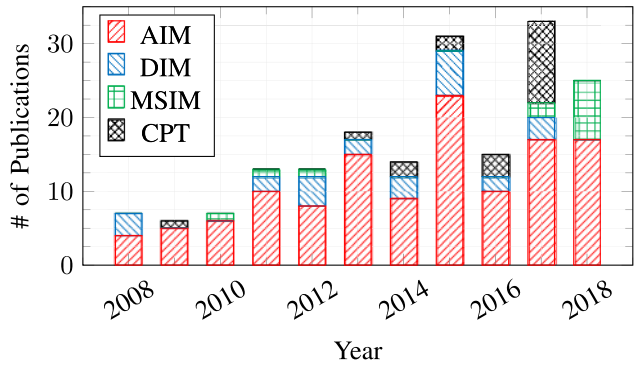

Fig. 10. Interference mitigation publications published in the last years (conferences: ISSCC, RFIC, ESSCIRC, ASILOMAR, and VTC; journals: JSSC, T-MTT, and T-CAS-I/II).

concepts are used to reduce unavoidable crosstalk to a minimum.

To support a variety of different CA combinations and LTE bands, a multitude of different oscillators is required. Frequency planning is used to simplify the synthesizer realization and also to reduce interference scenarios [40]. For example, the divider ratio following the oscillator can be changed to move a potential spur away from the BB [40]. Another approach is to shift the LO frequency to move the interfering signal away from the desired BB signal [2]. This low-IF approach requires a good image rejection ratio (IRR) and increases the power consumption because of the wider BW of the ADC.

Also, eight-shape inductors are used to reduce the coupling [41]. Below the inductors, shields can be inserted to improve their quality factors and prevent the substrate from coupling, but eddy currents have to be suppressed in order to manage a loss in quality factor. In LO distribution lines, isolation layers are placed to reduce the coupling. In the design process, triple-well devices can also be used (if available) and wherever possible differential signals are selected in building blocks. The supply lines of the different buildings blocks are separated to reduce crosstalk via supply lines [11].

To reduce interference scenarios imposed due to mechanisms of Type H, one evident approach is to improve the linearity of power amplifier drivers (PADs). An improvement of linearity comes with the cost of increased power consumption, which is typically tried to be avoided in cellular systems [19].

In commercial FDD systems, acoustic filters are used to connect the transmitter and receiver to the antenna. These filters provide high isolation with low loss [42]. To isolate the TX and RX channels from each other, duplex filters (constructed out of two or more optimized filters) are used, which should provide at least 55 dB of isolation [43]. To allow transition between passband and stopband of the filter, the gap between TX and RX frequencies has to be wide enough. In addition, since the frequency response of these filters depends on the material properties and physical dimensions, the center frequency is fixed, requiring a multitude of filters to support all required LTE bands. The need to have dedicated filtering components for each band drives the overall system cost and complexity of the system [44]. Tunable RF filters would be preferred, but due to their reduced attenuation in their stopbands and the increased insertion loss, they are not used in commercial designs so far. To further improve the isolation, the RF path can use interstage filters, but this approach is usually not desired because of the high number of additional filters.

Several RX-side techniques are possible to improve interference performance. Current-mode processing in the mixer (and possibly other blocks) is beneficial due to lower voltage swings and higher linearity [28]. Getting rid of low-noise amplifiers (LNAs) altogether results in mixer-first approaches, achieving excellent linearity but having potential issues with reduced sensitivity [45]. In [11], interference could be significantly reduced by using a direct-conversion path and a double-conversion path in parallel, thereby avoiding interference although LO leakage is present. Another tactic is described in [19]. Here, by moving the muxing away from the LO chain and into the BB, a high level of isolation between the LO signals is achieved.

Different TX-side techniques can be applied to reduce interference. The harmonic-rejection PA has been proposed to reduce the PA output harmonics (Type D) [30], [46]–[49]. Multiple parallel drive stages are combined with different gain and phase ratios to suppress certain harmonics. To reduce the TX band noise (Type B), the DAC resolution is increased. Different TX architectures have been proposed to reduce the band noise at a programmable offset [50]. Here, the quantization noise is shaped to reduce the band noise in the duplex distance of the TX signal.

B. Analog Interference Mitigation

AIM has the benefit to be area efficient, amenable to silicon integration, and to provide a high amount of cancellation over a wide tuning range. Unfortunately, added noise and distortion by the cancellation architecture is degrading the receiver performance and also wideband cancellation is often challenging to implement, especially on-chip without external components [51].

One common type of AIM for interference of Types A, C, and F are TX SI canceler. These architectures use a replica signal of the TX as input and try to recreate the self-interfering signal by using several components, such as attenuators, phase shifters, or delays. To model the time-varying behavior of the TX–RX leakage channel, adaptive algorithms control these components with extra reference signals [52]. An ideal integrated TX SI canceler should introduce minimal noise in the RX path. A minimal loading of the TX/PA output is also desired to reduce output power loss and efficiency degradation. In addition, also the total silicon area of the cancellation system should be small. Finally, adequate cancellation performance is required to relax the receiver linearity and selectivity performance [5].

AIM TX SI canceler can be categorized according to where they tap the TX reference signal and where the cancellation signal is subsequently inserted into the RX chain. This is shown in Fig. 9. Reported in the literature are BB and RF tapping. RF approaches have the benefit that nonlinear distortion and noise introduced by the transmitter can be mitigated. As shown in Fig. 11, to generate the cancellation signal, a coupler is used to generate a copy of the TX signal and dedicated RF components are used to adjust the delay and attenuation of the cancellation signal [5]. These RF components can be categorized into single-tap and multi-tap architectures. Single-tap designs are easy to implement but are limited in their amount of cancellation, narrow operational BW, and ability to address reflection paths from the environment. In contrast, multitap designs can achieve a high cancellation performance in multipath environments in a wide operational BW by accurately emulating the SI channel with the correct group delay, attenuation, and phase shift. Because of the drastically increased hardware complexity and increased number of tuning algorithms, this type is challenging to implement in commercial designs. Equalization in the frequency domain is also possible by using N-path filter concepts [53]. BB-tapping approaches use the BB TX signal to generate the cancellation signal. Digital filters are

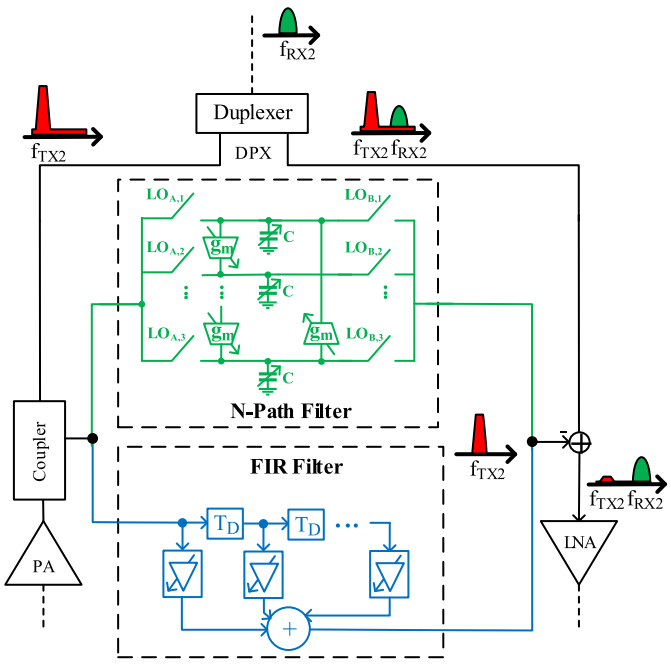

Fig. 11. Analog SI canceler approaches including N-path or FIR filter (for Types A, C, and F).

used to model the TX–RX leakage channel and are, therefore, categorized as MSIM approaches, which are described in more detail in Section IV-D. The injection of the cancellation signal should be close to the beginning of the RX chain to reduce the linearity and blocker requirements. When injecting the signal before the LNA, the noise introduced by the canceler should be minimal. This noise requirement can be relaxed if the cancellation is applied after the LNA. A cancellation after the mixing stage has the benefit that a low-frequency implementation of a more complex cancellation filter is possible [5].

Harmonic rejection mixing (HRM) in the receiver is an approach to mitigate interference of Types D–F. As shown in Fig. 12(a), with this approach, the mixing stage is designed to ensure that the interfering signals near the harmonics of the LO do not translate to BB. The most common approach is to utilize a discrete-level approximation of a sine wave to reduce the harmonic response of the mixing stage. The achievable performance is limited by the gain and phase mismatches along the multiple paths of the HRM. In addition, also the increased power in the LO generator and mixer circuits and the overall increase in complexity have to be considered, especially when the HRM architecture has to be implemented for multiple RX paths in a CA transceiver [54].

To enable high-Q on-chip filtering, N-path (or often called N-phase) filters are of paramount importance. With this technique, interference of Types A, C, D, and F can be mitigated. The benefits of this approach are that these filters are widely programmable, have high-Q values and excellent linearity, and are amenable to silicon integration. Therefore, high filter performance like with surface acoustic wave (SAW) or bulk acoustic wave (BAW) filters is achieved by reducing the area consumption and overall costs of RF solutions at the same time [55]–[57]. In addition, this approach also benefits from

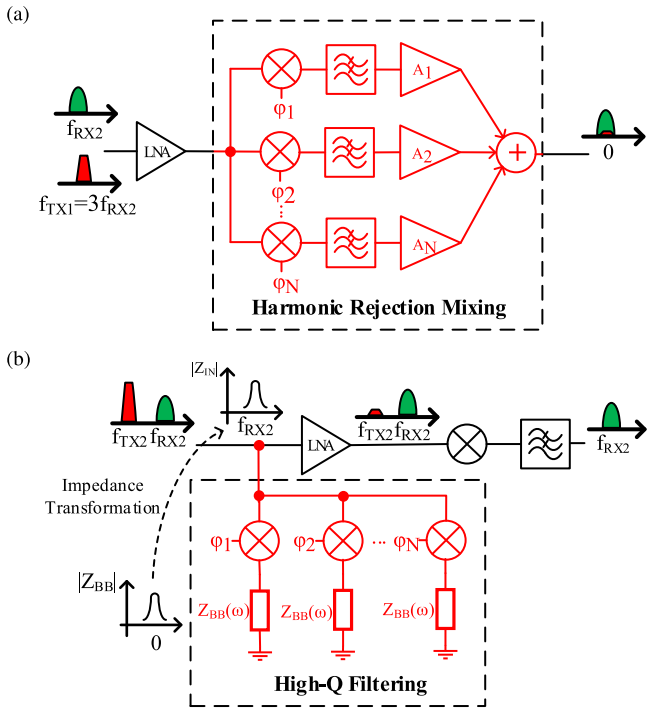

Fig. 12. AIM using (a) HRM (for Types C, D, and F) and (b) high-Q filtering (for Types A, C, D, and F).

process scaling, providing better switches and a lower power clock generator.

N-path filters exploit the linear time-variant behavior of switch RC circuits and the reciprocal behavior of passive mixers. An incoming RF signal is downconverted, filtered, and then upconverted again to the RF frequency. The BB filter behavior is shifted by the switching frequency of the filter, thereby defining its center frequency. This behavior [58] is shown in Fig. 12(b) and described by

$$Z_{\mathrm{IN}}(\omega) \cong R_{\mathrm{SW}} + \frac{N}{\pi^2}\sin^2\left(\frac{\pi}{N}\right) \times [Z_{\mathrm{BB}}(\omega-\omega_{\mathrm{LO}}) + Z_{\mathrm{BB}}(\omega+\omega_{\mathrm{LO}})] \quad (9)$$

where R_{SW} is the switch resistance, N is the number of paths, Z_{BB} is the BB filter impedance, and Z_{IN} is the input impedance of the high-Q filter. Receivers deploying this architecture in front of the LNA use an AUX path to deflect blockers from the main RX path. Mitigating the interfering signal at the input results in good blocker tolerance. Generally, the switch resistance should be much smaller than the source resistance to achieve an excellent filter performance by letting the BB capacitors of the filter shunt all interfering signals to ground. To reduce the impact of the switching resistance on the cancellation performance, N-path filters can also be combined with an LNA in a parallel [59] or a succeeding fashion [60]. This approach is only acceptable if the interference power is below a certain value that is not saturating the LNA. To reduce the "rounded filter shape," two N-path filters can be used in parallel with shifted center frequency [55].

The improved filter performance comes at the cost of a degraded overall noise and third-order intercept point (IP3) performance. Also, most of the reported architectures can only use this approach in the microwave bands with large duplex distances [61]. To achieve good filtering performance, the switching resistance should be low, which is achieved by using large switches. Because of the mismatch between the switches, strong LO leakage is introduced, which has to be below the spurious emission requirements defined by the 3GPP [62]. In addition, large capacitors are required to achieve narrowband filtering due to the small source impedance [63]. To reduce LO leakage and reduce the size of the capacitors, filtering can be performed after the LNA. However, the filtering performance is then degraded as a tradeoff [63]. Receiver LO PN requirements can only be relaxed with this approach if a cleaner LO signal is used for the AUX path in comparison to the main path [64].

To reduce receiver degradation due to interference described by Type C, the transmitter-induced PN has to be mitigated. The first evident approach is to reduce the PN of LC oscillators, which usually can only be improved by consuming more power [65]. To break this inherent tradeoff, PN cancellation techniques have been proposed. In [66], the symmetry of the LO PN is used to perform a cancellation by using a dedicated AUX path. A replica of the RM is created and used to subtract the interference from the main path.

Translational loops can be used to mitigate interference of Types A–D and F. As shown in Fig. 13, the two approaches are feedforward and feedback loops. In translational loops, the RF signal is first downconverted, filtered. and then upconverted in a parallel AUX path to mitigate the interfering signal from the main RX path. With feedforward architectures, the high-pass filtered interfering signal is canceled after the LNA by inserting it with opposite phase. Using a feedforward approach imposes stringent linearity specification on the cancellation circuit due to the cancellation after the LNA. In addition, the cancellation BW is limited due to the frequency-dependent phase shift in the high-pass filter. Feedback translational loops create an input impedance match at the input of the LNA in the desired frequency band. Here, the RF signal is downconverted to BB, low-pass filtered, and then upconverted again [67]. The selectivity can be configured with the BW of the low-pass filter. Due to the filtering in front of the LNA, the linearity requirement is relaxed in comparison to feedforward architectures. In addition, feedback architectures are more robust against nonidealities in the translational loop since the feedback path automatically addresses this issue [68], [69].

C. Digital Interference Mitigation

DIM solely operates in the BB and thus benefits from all advantages of fully digital hardware, such as simplified design and verification, and area savings directly proportional to the shrinking of semiconductor technology nodes. If the application enables the usage of digital signal processors instead of dedicated hardware elements, even online reprogrammability is possible. The increased flexibility of DIM compared with other mitigation techniques may outweigh its inferior cancellation performance and reliability [70].

As the cancellation is done in BB, the whole leakage channel has to be replicated. Therefore, a detailed parametric model is necessary for many standard DIM approaches. A number of

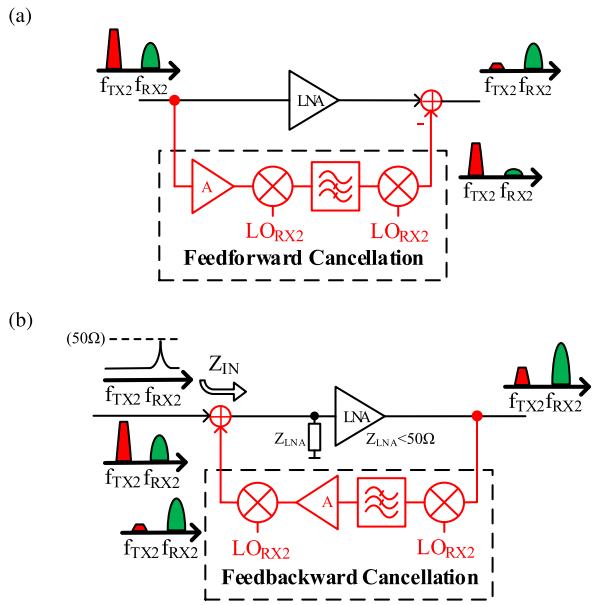

Fig. 13. Translational loops (for Types A–D and F). (a) Feedforward and (b) feedback architectures.

model parameters are chosen as a tradeoff between opposing factors, such as cancellation performance, convergence rate, and hardware complexity. Due to manufacturing tolerances or changing operation conditions, many parameters are unknown and consequently need to be estimated. The underlying parameter estimation process is often decoupled from the cancellation structure and is mostly a variant of a block or sample adaptive optimization algorithm, which is tailored to a specific interference effect. Choosing the algorithm is a tradeoff between mitigation performance and hardware complexity. Especially with the increasing BWs of LTE-A and 5G NR, real-time processing of the BB data streams poses a significant challenge on the implementations. Within these constraints, the sample adaptive least-mean squares (LMS) algorithm [71] is one reasonable option. It features comparably low area and power requirements; however, it suffers from slow convergence rate and low steady-state cancellation caused by unfavorable statistical properties of LTE signals. Although some improvements addressing this issues were proposed [72], a significantly higher performance can only be achieved by employing the recursive least-squares (RLS) algorithm [71], [73] instead. By computing a least-squares (LS) solution over a sliding window of input data, it provides inherent decorrelation. This leads to extremely fast convergence even for LTE signals. The hardware complexity of the RLS algorithm shows a quadratic dependence on the parameter count, which renders it unfeasible for complex models. A seldomly used tradeoff between LMS algorithm and RLS algorithm is the affine projection algorithm (APA) [71], where the cancellation performance and hardware complexity can be adjusted to the actual needs by means of a hyperparameter. If the parameters of an interference effect change slowly, another alternative is the block-based LS algorithm [71], which features excellent performance at very high hardware costs.

Along with the estimation algorithm, also the cancellation structure is adapted to the targeted effect. Fig. 14 depicts

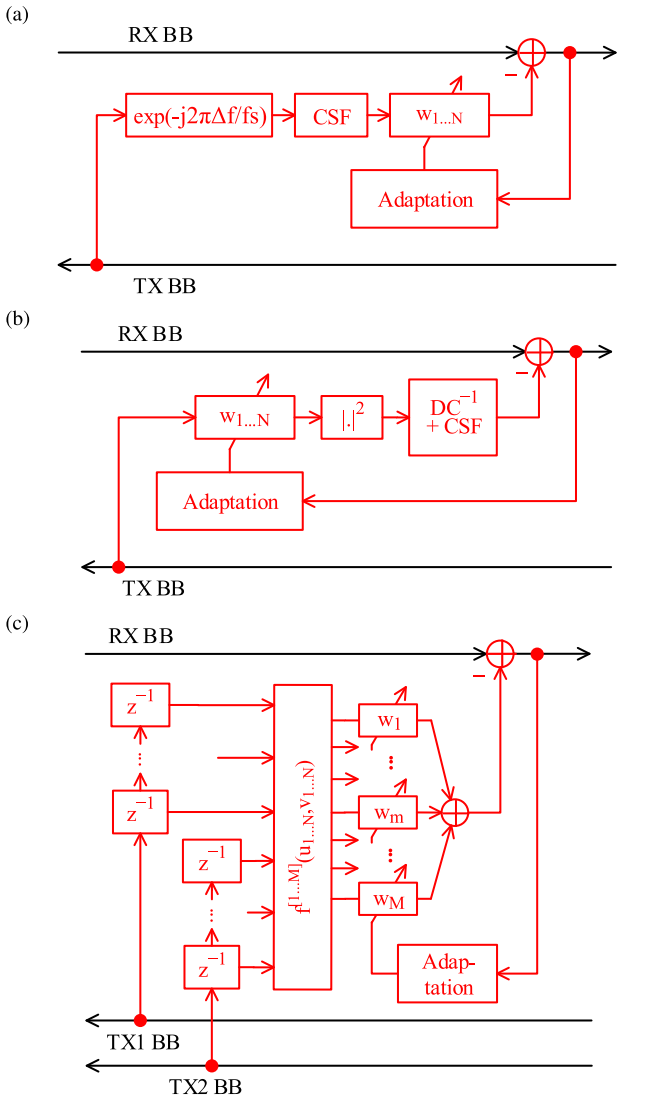

Fig. 14. Interferences mitigation structures for (a) Type F, (b) Type A, and (c) Type G.

examples for the main categories of cancellation structures, all based on a feedback loop. The approach in Fig. 14(a) is able to mitigate interference of Type F [74]. Usually, the spur frequency and RX carrier frequency do not match. Thus, a frequency shift and the RX channel select filter is applied to the TX BB data. The resulting stream is the input of a complex FIR filter with adjustable coefficients, which models the duplexer impulse response. The structure in Fig. 14(b) targets a subset of effects of Type A [34], namely the second-order IM distortions. Again, an adjustable FIR filter models the duplexer, while a nonlinear element at the output replicates the IM product. The dc cancellation and channel select filtering in the RX path are also modeled. In the literature, this scheme is known as the Wiener model [75]. As the feedback loop contains a nonlinear element and a linear shift invariant (LSI) system with nonconstant group delay, the estimation process is considerably difficult. This results in a comparably slow convergence rate. Fig. 14(c) shows a cancellation approach for the interference effect of Type G, as presented in [76]. In this so-called parallel Hammerstein

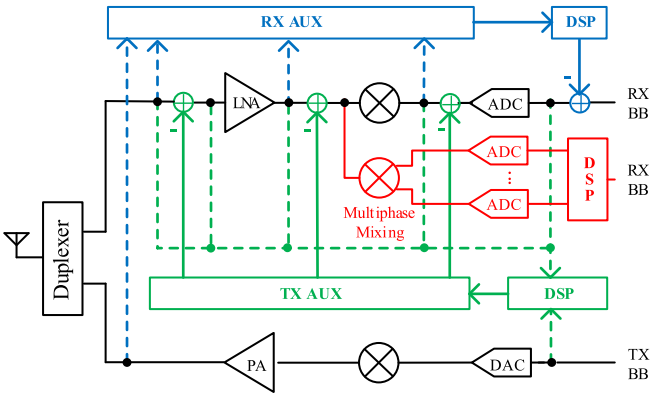

Fig. 15. MSIM approaches categorized.

model [77], a static nonlinearity is placed at the input of an adaptive linear combiner. In the nonlinear element, all possible intermodulation products between two TX streams are computed. The individual terms are weighted and summed up replicating not only the TX intermodulation process but also the duplexer impulse response and even PA nonlinearities in the transmitters. Due to the complexity of the model, the LMS algorithm may not be usable for this cancellation scheme.

Beyond the discussed standard approaches, recent publications explore the applicability of machine learning for DIM. Reference [78] compares a polynomial and a neural network canceller for mitigation of I/Q imbalance and PA nonlinearities of the transmitter. At significantly lower computational complexity, the machine-learning algorithm provides the same cancellation performance as the polynomial Hammerstein model.

D. Mixed-Signal Interference Mitigation

MSIM combines the reliability of analog cancellation and the flexibility of digital cancellation. The overall complexity of AIM can be reduced with the flexibility and effectiveness of the usage of digital components, such as FIR filters. MSIM approaches have a good cancellation performance over a wide modulated BW. In comparison to DIM approaches, they can also achieve a good performance in nonlinear systems. Several MSIM approaches have been proposed in the literature. Fig. 15 shows the most common approaches, which can be categorized into three main groups.

Similar to the AIM TX SI canceler approaches, the BB TX signal can be used in order to generate a cancellation signal. A filter is implemented in the digital domain to model the TX–RX leakage channel. The delay and amplitude, including multipath scenarios, can be easily modeled in the digital domain. To route the cancellation signal to the RX chain, a dedicated AUX path is implemented. The cancellation itself can be performed at different points of the RX chain. Mitigating the interfering signal prior to the receiver LNA has the benefit of preventing the LNA or ADC from saturating and to avoid receiver desensitization. As presented in [79], the AIM TX SI canceler approach can be combined with this MSIM approach. The direct leakage SI component is targeted with the AIM TX SI canceler, while the other one is used to suppress interfering signals resulting from antenna reflections. In [39], a traditional AIM TX SI canceler with an RF vector multiplier was proposed that is supported by a digital FIR filter, which results in good cancellation performance over a wide modulation BW.

A disadvantage of this approach is that the AUX and main TX path are not coherent. The nonlinear behavior of the mixer and PA stage results in unwanted harmonics and IM products that are not considered. In addition, the quantization noise of the DAC, the noise contributing of active circuits in the TX chain, and the PN of the LO signals are further limiting the cancellation performance [79], [80]. In [81], these disadvantages have been targeted using a closed-loop parameter learning approach with a nonlinear cancellation filter that estimates the nonlinear behavior of the PA with memory.

For the cancellation of interfering signals of Types A, B, D, and F, MSIM approaches using a dedicated AUX receiver have been proposed. Sharing the same idea as DIM techniques, these approaches differ by the fact that the reference signal provided by the AUX receiver is used for the cancellation of the interference. Therefore, this concept mitigates the interference induced by the transmitter and not the TX interference itself. The main advantage of tapping the interference signal at some point of the RX chain is taking the transmitter nonlinearities and the duplexer frequency response out of the estimation process, resulting in a reliable cancellation and fast convergence times as required for 5G NR transceivers. Moreover, in comparison to other approaches, MSIM can also be used for nonTX-related interfering signals, for example, Wi-Fi coexistence, 5G NR, dual-receive dual-standby (DRDS), and license-assisted access (LAA) interfering signals. In [82], three different types of AUX receiver-based MSIM approaches have been presented, as shown in Fig. 16(a)–(c). Tapping before the LNA is the most robust option, which is not degrading the sensitivity of the receiver. The AUX LO can be tapped from the main receiver LO or can be driven by a dedicated LO tuned to the TX frequency. First, one does not require an additional PLL, but requires a wideband ADC with sufficient signal-to-noise-ratio (SNR) and a frequency shift in the digital domain. Tapping the signal after the mixing stage has the benefit of having the most hardware reuse. Unfortunately, the main RX path sensitivity is degraded by the noise of the AUX path. In [32], another MSIM concept is proposed as shown in Fig. 16(d), targeting interference of Type F. In comparison to the previous work, the proposed system is able to cancel TX-leakage-induced modulated spurs or any other possible unknown blocker present at the LNA input. Modulated spurs, including their TX/RX LO PN-modulated components can be mitigated. This concept is further extended in [83], targeting the cancellation of multiple, possibly unknown modulated spur interfering signals.

Another MSIM approach using an AUX receiver was proposed in [42] targeting interference of Types A–C. Here, an AIM TX SI canceller is used to reduce the TX leakage power to avoid nonlinear and reciprocal mixing effects. In addition, the TX noise is sensed at the output of the PA with an AUX RX path providing a BB copy of the TX noise, allowing to restore the RX sensitivity in the digital

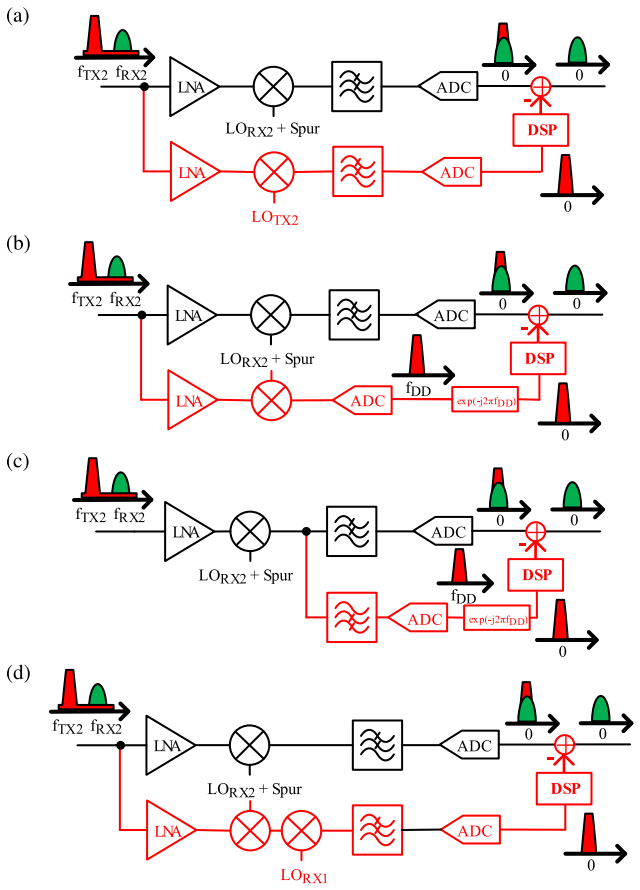

Fig. 16. Overview of different MSIM (for Types A, B, D, and F). (a) Tapping before the LNA with dedicated LO signal. (b) Tapping before the LNA with reusing the LO signal of the main path. (c) Tapping after the mixing-stage. (d) Tapping before the LNA with serial-mixing structure [82], [83].

domain. Reference [28] focuses on the mitigation of Type A interfering signals. Two nonlinear RX AUX chains are used to generate reference signals for even- and odd-order IM products. Using these reference signals in the digital domain enables the cancellation of higher order IM distortion products.

The third category is similar to the HRM approach described in Section IV-B. In [84], multiple RX paths and LO phases are used to suppress harmonics or IM products. In the digital domain, a multitude of BB streams are processed with a digital distortion equalizer to suppress harmonic mixing and IM products. Yet, another architecture was presented in [85]. Two alternative HRM techniques achieved a high amount of HR robust to mismatch. An analog two-stage polyphase HRM concept is combined with an MSIM-based approach. Another interesting approach aimed at improving the IM performance was presented in [86]. Again, a multitude of RX paths is used, and each main RX path uses a different phase of a pseudo-random bit sequence. Similar to compressive-sensing-based systems, the RF signal is reconstructed in the digital domain afterward, whereby no assumption of sparsity is required.

V. Conclusion

LTE-A and 5G NR CA transceivers use new techniques, such as CA, HOM, and MIMO, to attain several Gb/s in peak data rates. Commercial UEs require the support of 5G NR and legacy protocols simultaneously and desire a single-chip RF design for a small form factor and low power consumption. These trends result in a drastic increase in sensitivity degradation due to interfering signals, making SI management a crucial part of the state-of-the-art transceiver design. This article provides a guide and starting point on SI management by presenting a comprehensive overview of SI in LTE-A and 5G NR CA transceivers. A taxonomy of SI mitigation architectures is provided by categorizing them into CPT, AIM, DIM, and MSIM techniques and comparing their strengths and weaknesses. This taxonomy shall help the reader in the transceiver design process to choose an adequate technique considering factors, such as power consumption, chip area, increased complexity, or cancellation performance.

Acknowledgment

The authors would like to thank DMCE GmbH & Co KG as part of Intel for supporting this work carried out at the Christian Doppler Laboratory for Digitally Assisted RF Transceivers for Future Mobile Communications.

References

[1] Ericsson. *Ericsson Mobility Report*. Accessed: Jul. 1, 2019. [Online]. Available: https://www.ericsson.com/en/mobility-report

[2] C.-S. Chiu *et al.*, "A 40 nm low-power transceiver for LTE-A carrier aggregation," in *IEEE Int. Solid-State Circuits Conf. (ISSCC) Dig. Tech. Papers*, Feb. 2017, pp. 130–131.

[3] K.-D. Chu, T. Zhang, F. Yin, and J. C. Rudell, "Self-interference (SI) cancellation in full-duplex (FD) radios," *IEEE RFIC Virtual J.*, no. 9, Dec. 2017. [Online]. Available: https://ieeexplore.ieee.org/virtual-journals/rfic/issue/9

[4] E. Klumperink and A. Molnar, "Interference robust, flexible radio receivers in CMOS," *IEEE RFIC Virtual J.*, no. 6, Oct. 2014. [Online]. Available: https://ieeexplore.ieee.org/virtual-journals/rfic/issue/6/

[5] M. Katanbaf, K.-D. Chu, T. Zhang, C. Su, and J. C. Rudell, "Two-way traffic ahead," *IEEE Microw. Mag.*, vol. 20, no. 2, pp. 22–35, Feb. 2019.

[6] I. Brodsky, J. Brand, and M. Jain, "Freedom of frequency: How the quest for in-band full-duplex led to a breakthrough in filter design," *IEEE Microw. Mag.*, vol. 20, no. 2, pp. 36–43, Jan. 2019.

[7] C. D. Nwankwo, L. Zhang, A. Quddus, M. A. Imran, and R. Tafazolli, "A survey of self-interference management techniques for single frequency full duplex systems," *IEEE Access*, vol. 6, pp. 30242–30268, Nov. 2018.

[8] *Evolved Universal Terrestrial Radio Access (E-UTRA); User Equipment (UE) Radio Transmission and Reception*, document 3GPP TS 136 101, V16.1.0, Mar. 2019. [Online]. Available: http://www.3gpp.org/ftp//Specs/archive/36_series/36.101/36101-g10.zip

[9] H. Pretl *et al.*, "From microwatt to gigabit: Challenges of modern radio design," *Elektrotechnik Informationstechnik*, vol. 135, no. 1, pp. 76–82, Feb. 2018.

[10] *Evolved Universal Terrestrial Radio Access (LTE): User Equipment (UE) Radio Transmission and Reception*, document 3GPP TS 38.101-3, V15.5.0, Apr. 2019. [Online]. Available: http://www.3gpp.org/ftp//Specs/archive/38_series/38.101-3/38101-3-f50.zip

[11] X. Yi *et al.*, "A 65 nm CMOS carrier-aggregation transceiver for IEEE 802.11 WLAN applications," in *Proc. IEEE Radio Freq. Integr Circuits Symp. (RFIC)*, May 2016, pp. 67–70.

[12] L. Sundstrom *et al.*, "Complex IF harmonic rejection mixer for non-contiguous dual carrier reception in 65 nm CMOS," *IEEE J. Solid-State Circuits*, vol. 48, no. 7, pp. 1659–1668, Mar. 2013.

[13] C.-C. Tang *et al.*, "An LTE-A multimode multiband RF transceiver with 4RX/2TX inter-band carrier aggregation, 2-carrier 4×4 MIMO with 256 QAM and HPUE capability in 28 nm CMOS," in *IEEE Int. Solid-State Circuits Conf. (ISSCC) Dig. Tech. Papers*, Feb. 2019, pp. 350–352.

[14] J. Lee *et al.*, "A sub-6 GHz 5G new radio RF transceiver supporting EN-DC with 3.15 Gb/s DL and 1.27 Gb/s UL in 14 nm FinFET CMOS," in *IEEE Int. Solid-State Circuits Conf. (ISSCC) Dig. Tech. Papers*, Feb. 2019, pp. 354–356.

[15] M. Mikhemar *et al.*, "A Rel-12 2G/3G/LTE-advanced 3CC cellular receiver," *IEEE J. Solid-State Circuits*, vol. 51, no. 5, pp. 1066–1079, May 2016.

[16] Y. Kim *et al.*, "An RF receiver for multi-band inter- and intra-band carrier aggregation," in *Proc. IEEE Radio Freq. Integr Circuits Symp. (RFIC)*, May 2016, pp. 79–82.

[17] J. Zhu and P. R. Kinget, "A very-low-noise frequency-translational quadrature-hybrid receiver for carrier aggregation," in *IEEE Int. Solid-State Circuits Conf. (ISSCC) Dig. Tech. Papers*, Jan. 2016, pp. 168–169.

[18] T.-H. Wu *et al.*, "A 40 nm 4-downlink and 2-uplink RF transceiver supporting LTE-Advanced carrier aggregation," in *Proc. IEEE Radio Freq. Integr Circuits Symp. (RFIC)*, Jun. 2018, pp. 316–319.

[19] B. Mohammadi *et al.*, "A rel-12 2G/3G/LTE-advanced 2CC transmitter," *IEEE J. Solid-State Circuits*, vol. 51, no. 5, pp. 1080–1095, May 2016.

[20] N. Klemmer *et al.*, "A 45 nm CMOS RF-to-bits LTE/WCDMA FDD/TDD 2×2 MIMO base-station transceiver SoC with 200 MHz RF bandwidth," in *IEEE Int. Solid-State Circuits Conf. (ISSCC) Dig. Tech. Papers*, Jan. 2016, pp. 164–165.

[21] M. Fulde *et al.*, "A digital multimode polar transmitter supporting 40 MHz LTE carrier aggregation in 28 nm CMOS," in *IEEE Int. Solid-State Circuits Conf. (ISSCC) Dig. Tech. Papers*, Feb. 2017, pp. 218–219.

[22] B. Jann *et al.*, "A 5G sub-6 GHz zero-IF and mm-wave IF transceiver with MIMO and carrier aggregation," in *IEEE Int. Solid-State Circuits Conf. (ISSCC) Dig. Tech. Papers*, Feb. 2019, pp. 352–354.

[23] S.-C. Hwu and B. Razavi, "A receiver architecture for intra-band carrier aggregation," in *Proc. Symp. VLSI Circuits*, Jun. 2014, pp. 1–2.

[24] R. Chen and H. Hashemi, "Dual-carrier aggregation receiver with reconfigurable front-end RF signal conditioning," *IEEE J. Solid-State Circuits*, vol. 50, no. 8, pp. 1874–1888, Aug. 2015.

[25] D. Regev, S. Shilo, D. Ezri, and J. Zhang, "A robust reconfigurable front-end for non-contiguous multi-channel carrier aggregation receivers," in *Proc. IEEE Radio Freq. Integr Circuits Symp. (RFIC)*, Jun. 2018, pp. 8–11.

[26] S. C. Hwu and B. Razavi, "An RF receiver for intra-band carrier aggregation," *IEEE J. Solid-State Circuits*, vol. 50, no. 4, pp. 946–961, Apr. 2015.

[27] E. Ahmed and A. M. Eltawil, "All-digital self-interference cancellation technique for full-duplex systems," *IEEE Trans. Wireless Commun.*, vol. 14, no. 7, pp. 3519–3532, Jul. 2015.

[28] E. A. Keehr and A. Hajimiri, "Successive regeneration and adaptive cancellation of higher order intermodulation products in RF receivers," *IEEE Trans. Microw. Theory Techn.*, vol. 59, no. 5, pp. 1379–1396, Mar. 2011.

[29] A. Kiayani, L. Anttila, and M. Valkama, "Modeling and dynamic cancellation of TX-RX leakage in FDD transceivers," in *Proc. IEEE 56th Int. Midwest Symp. Circuits Syst. (MWSCAS)*, Aug. 2013, pp. 1089–1094.

[30] T. Zhang, Y. Chen, C. Huang, and J. C. Rudell, "A low-noise reconfigurable full-duplex front-end with self-interference cancellation and harmonic-rejection power amplifier for low power radio applications," in *Proc. IEEE Eur. Solid-State Circuits Conf. (ESSCIRC)*, Sep. 2017, pp. 336–339.

[31] P. Rakers *et al.*, "Multi-mode cellular transceivers for LTE and LTE-Advanced," in *Proc. IEEE Custom Int. Circuits Conf. (CICC)*, Sep. 2014, pp. 1–8.

[32] S. Sadjina, R. S. Kanumalli, A. Gebhard, K. Dufrêne, M. Huemer, and H. Pretl, "A mixed-signal circuit technique for cancellation of interferers modulated by LO phase-noise in 4G/5G CA transceivers," *IEEE Trans. Circuits Syst. I, Reg. Papers*, vol. 65, no. 11, pp. 3745–3755, Nov. 2018.

[33] H.-T. Dabag, H. Gheidi, S. Farsi, P. Gudem, and P. M. Asbeck, "All-digital cancellation technique to mitigate receiver desensitization in uplink carrier aggregation in cellular handsets," *IEEE Trans. Microw. Theory Techn.*, vol. 61, no. 12, pp. 4754–4765, Nov. 2013.

[34] A. Gebhard, C. Motz, R. Kanumalli, H. Pretl, and M. Huemer, "Nonlinear least-mean-squares type algorithm for second-order interference cancellation in LTE-A RF transceivers," in *Proc. 51st Asilomar Conf. Signals, Syst., Comput.*, Oct. 2017, pp. 802–807.

[35] M. Omer, R. Rimini, P. Heidmann, and J. S. Kenney, "All digital compensation scheme for spur induced transmit self-jamming in multi-receiver RF frond-ends," in *IEEE MTT-S Int. Microw. Symp. Dig.*, Jun. 2012, pp. 1–3.

[36] M. Mikhemar, D. Murphy, A. Mirzaei, and H. Darabi, "A cancellation technique for reciprocal-mixing caused by phase noise and spurs," *IEEE J. Solid-State Circuits*, vol. 48, no. 12, pp. 3080–3089, Dec. 2013.

[37] A. Gebhard, S. Sadjina, S. Tertinek, K. Dufrêne, H. Pretl, and M. Huemer, "A harmonic rejection strategy for 25% duty-cycle IQ-mixers using digital-to-time converters," *IEEE Trans. Circuits Syst. II, Exp. Briefs*, to be published, doi: 10.1109/TCSII.2019.2937654.

[38] R. S. Kanumalli, A. Gebhard, A. Elmaghraby, A. Mayer, D. Schwartz, and M. Huemer, "Active digital cancellation of transmitter induced modulated spur interference in 4G LTE carrier aggregation transceivers," in *Proc. IEEE Veh. Technol. Conf. (VTC Spring)*, May 2016, pp. 1–5.

[39] B. King, J. Xia, and S. Boumaiza, "Digitally assisted RF-analog self interference cancellation for wideband full-duplex radios," *IEEE Trans. Circuits Syst. II, Exp. Briefs*, vol. 65, no. 3, pp. 336–340, Mar. 2018.

[40] C. Mishra, A. Valdes-Garcia, F. Bahmani, A. Batra, E. Sánchez-Sinencio, and J. Silva-Martinez, "Frequency planning and synthesizer architectures for multiband OFDM UWB radios," *IEEE Trans. Microw. Theory Techn.*, vol. 53, no. 12, pp. 3744–3755, Dec. 2005.

[41] A. Poon, A. Chang, H. Samavati, and S. S. Wong, "Reduction of inductive crosstalk using quadrupole inductors," *IEEE J. Solid-State Circuits*, vol. 44, no. 6, pp. 1756–1764, Jun. 2009.

[42] D. Montanari *et al.*, "An FDD wireless diversity receiver with transmitter leakage cancellation in transmit and receive bands," *IEEE J. Solid-State Circuits*, vol. 53, no. 7, pp. 1945–1959, Apr. 2018.

[43] R. Vazny, W. Schelmbauer, H. Pretl, S. Herzinger, and R. Weigel, "An interstage filter-free mobile radio receiver with integrated TX leakage filtering," in *Proc. IEEE Radio Freq. Integr. Circuits Symp. (RFIC)*, May 2010, pp. 21–24.

[44] M. Valkama, M. Renfors, and V. Koivunen, "Advanced methods for I/Q imbalance compensation in communication receivers," *IEEE Trans. Signal Process.*, vol. 49, no. 10, pp. 2335–2344, Oct. 2001.

[45] D. Murphy *et al.*, "A blocker-tolerant, noise-cancelling receiver suitable for wideband wireless applications," *IEEE J. Solid-State Circuits*, vol. 47, no. 12, pp. 2943–2963, Dec. 2012.

[46] S. Subhan, E. A. Klumperink, A. Ghaffari, G. J. Wienk, and B. Nauta, "A 100–800 MHz 8-path polyphase transmitter with mixer duty-cycle control achieving <-40 dBc for all harmonics," *IEEE J. Solid-State Circuits*, vol. 49, no. 3, pp. 595–607, Mar. 2014.

[47] J. A. Weldon *et al.*, "A 1.75 GHz highly-integrated narrow-band CMOS transmitter with harmonic-rejection mixers," in *IEEE Int. Solid-State Circuits Conf. (ISSCC) Dig. Tech. Papers*, Feb. 2001, pp. 160–161.

[48] E. Mensink, E. A. M. Klumperink, and B. Nauta, "Distortion cancellation by polyphase multipath circuits," *IEEE Trans. Circuits Syst. I, Reg. Papers*, vol. 52, no. 9, pp. 1785–1794, Sep. 2005.

[49] R. Shrestha, E. A. M. Klumperink, E. Mensink, G. J. M. Wienk, and B. Nauta, "A polyphase multipath technique for software-defined radio transmitters," *IEEE J. Solid-State Circuits*, vol. 41, no. 12, pp. 2681–2692, Dec. 2006.

[50] E. Roverato *et al.*, "All-digital RF transmitter in 28 nm CMOS with programmable RX-band noise shaping," in *IEEE Int. Solid-State Circuits Conf. (ISSCC) Dig. Tech. Papers*, Feb. 2017, pp. 222–223.

[51] J. Zhou, A. Chakrabarti, P. R. Kinget, and H. Krishnaswamy, "Low-noise active cancellation of transmitter leakage and transmitter noise in broadband wireless receivers for FDD/Co-existence," *IEEE J. Solid-State Circuits*, vol. 49, no. 12, pp. 3046–3062, Dec. 2014.

[52] M. S. Sim, M. Chung, D. Kim, J. Chung, D. K. Kim, and C.-B. Chae, "Nonlinear self-interference cancellation for full-duplex radios: From link-level and system-level performance perspectives," *IEEE Commun. Mag.*, vol. 55, no. 9, pp. 158–167, Jun. 2017.

[53] J. Zhou, T.-H. Chuang, T. Dinc, and H. Krishnaswamy, "Integrated wideband self-interference cancellation in the RF domain for FDD and full-duplex wireless," *IEEE J. Solid-State Circuits*, vol. 50, no. 12, pp. 3015–3031, Dec. 2015.

[54] W. Namgoong, "Adaptive and robust digital harmonic-reject mixer with optimized local oscillator spacing," *IEEE Trans. Circuits Syst. I, Reg. Papers*, vol. 62, no. 2, pp. 580–589, Feb. 2015.

[55] E. A. M. Klumperink, H. J. Westerveld, and B. Nauta, "N-path filters and mixer-first receivers: A review," in *Proc. IEEE Custom Integr. Circuits Conf. (CICC)*, Apr. 2017, pp. 1–8.

[56] Y. Xu and P. R. Kinget, "A switched-capacitor RF front end with embedded programmable high-order filtering," *IEEE J. Solid-State Circuits*, vol. 51, no. 5, pp. 1154–1167, May 2016.

[57] L. Duipmans, R. E. Struiksma, E. A. M. Klumperink, B. Nauta, and F. E. V. Vliet, "Analysis of the signal transfer and folding in N-path filters with a series inductance," *IEEE Trans. Circuits Syst. I, Reg. Papers*, vol. 62, no. 1, pp. 263–272, Jan. 2015.

[58] A. Mirzaei, H. Darabi, and D. Murphy, "Architectural evolution of integrated M-phase high-Q bandpass filters," *IEEE Trans. Circuits Syst. I, Reg. Papers*, vol. 59, no. 1, pp. 52–65, Jan. 2012.

[59] J. W. Park and B. Razavi, "Channel selection at RF using Miller bandpass filters," *IEEE J. Solid-State Circuits*, vol. 49, no. 12, pp. 3063–3078, Dec. 2014.

[60] J. Borremans *et al.*, "A 40 nm CMOS highly linear 0.4-to-6 GHz receiver resilient to 0 dBm out-of-band blockers," in *IEEE Int. Solid-State Circuits Conf. (ISSCC) Dig. Tech. Papers*, Feb. 2011, pp. 62–64.

[61] Y. Zhang, N. Jiang, F. Huang, X. Tang, and X. You, "A fully integrated 300-MHz channel bandwidth 256 QAM transceiver with self-interference suppression in closely spaced channels at 6.5-GHz band," *IEEE Trans. Microw. Theory Techn.*, vol. 66, no. 11, pp. 4943–4954, Nov. 2018.

[62] H. Wang, Z. Wang, and P. Heydari, "A wideband blocker-tolerant receiver with high-Q RF-input selectivity and <−80 dBm LO leakage," in *IEEE Int. Solid-State Circuits Conf. (ISSCC) Dig. Tech. Papers*, Feb. 2019, pp. 450–451.

[63] Y. Xu, J. Zhu, and P. R. Kinget, "A blocker-tolerant RF front end with harmonic-rejecting N-path filtering," *IEEE J. Solid-State Circuits*, vol. 53, no. 2, pp. 327–339, Feb. 2018.

[64] A. Mirzaei, M. Mikhemar, D. Murphy, and H. Darabi, "A 2 dB NF receiver with 10 mA battery current suitable for coexistence applications," *IEEE J. Solid-State Circuits*, vol. 49, no. 4, pp. 972–983, Apr. 2014.

[65] M. Mikhemar, D. Murphy, A. Mirzaei, and H. Darabi, "A phase-noise and spur filtering technique using reciprocal-mixing cancellation," in *IEEE Int. Solid-State Circuits Conf. (ISSCC) Dig. Tech. Papers*, Feb. 2013, pp. 86–87.

[66] H. Wu, M. Mikhemar, D. Murphy, H. Darabi, and M.-C. F. Chang, "A blocker-tolerant inductor-less wideband receiver with phase and thermal noise cancellation," *IEEE J. Solid-State Circuits*, vol. 50, no. 12, pp. 2948–2964, Dec. 2015.

[67] T. Zhang, A. R. Suvarna, V. Bhagavatula, and J. C. Rudell, "An integrated CMOS passive self-interference mitigation technique for FDD radios," *IEEE J. Solid-State Circuits*, vol. 50, no. 5, pp. 1176–1188, May 2015.

[68] J. Zhu, H. Krishnaswamy, and P. R. Kinget, "Field-programmable LNAs with interferer-reflecting loop for input linearity enhancement," *IEEE J. Solid-State Circuits*, vol. 50, no. 2, pp. 556–572, Feb. 2015.

[69] A. Safarian, A. Shameli, A. Rofougaran, M. Rofougaran, and F. de Flaviis, "Integrated blocker filtering RF front ends," in *Proc. IEEE Radio Freq. Integr. Circuits Symp. (RFIC)*, Jun. 2007, pp. 13–16.

[70] R. S. Kanumalli and T. Buckel, "Digitally-intensive transceivers for future mobile communications—Emerging trends and challenges," *Elektrotechnik Informationstechnik*, vol. 135, no. 1, pp. 30–39, Feb. 2018.

[71] A. H. Sayed, *Fundamentals of Adaptive Filtering*. Hoboken, NJ, USA: Wiley, 2003.

[72] P. S. R. Diniz, *Adaptive Filtering: Algorithms and Practical Implementation*, 4th ed. New York, NY, USA: Springer, 2013.

[73] A. Gebhard *et al.*, "A robust nonlinear RLS type adaptive filter for second-order-intermodulation distortion cancellation in FDD LTE and 5G direct conversion transceivers," *IEEE Trans. Microw. Theory Techn.*, vol. 67, no. 5, pp. 1946–1961, May 2019.

[74] A. Gebhard, R. S. Kanumalli, B. Neurauter, and M. Huemer, "Adaptive self-interference cancelation in LTE-A carrier aggregation FDD direct-conversion transceivers," in *Proc. 9th IEEE Sensor Array Multichannel Signal Process. Workshop (SAM)*, Jul. 2016, pp. 1–5.

[75] T. Ogunfunmi, *Adaptive Nonlinear System Identification: The Volterra and Wiener Model Approaches*. New York, NY, USA: Springer, 2007.

[76] M. Z. Waheed, P. P. Campo, D. Korpi, A. Kiayani, L. Anttila, and M. Valkama, "Digital cancellation of passive intermodulation in FDD transceivers," in *Proc. IEEE Asilomar Conf. Signals, Syst., Comput. (ASILOMAR)*, Oct. 2018, pp. 1375–1381.

[77] M. Schoukens, R. Pintelon, and Y. Rolain, "Parametric identification of parallel Hammerstein systems," *IEEE Trans. Instrum. Meas.*, vol. 60, no. 12, pp. 3931–3938, Dec. 2011.

[78] A. Balatsoukas-Stimming, "Non-linear digital self-interference cancellation for in-band full-duplex radios using neural networks," in *Proc. IEEE Int. Workshop Signal Process. Adv. Wireless Commun. (SPAWC)*, Jun. 2018, pp. 1–5.

[79] Y. Liu, P. Roblin, X. Quan, W. Pan, S. Shao, and Y. Tang, "A full-duplex transceiver with two-stage analog cancellations for multipath self-interference," *IEEE Trans. Microw. Theory Techn.*, vol. 65, no. 12, pp. 5263–5273, Dec. 2017.

[80] D.-J. van den Broek, E. A. M. Klumperink, and B. Nauta, "An in-band full-duplex radio receiver with a passive vector modulator downmixer for self-interference cancellation," *IEEE J. Solid-State Circuits*, vol. 50, no. 12, pp. 3003–3014, Dec. 2015.

[81] A. Kiayani *et al.*, "Adaptive nonlinear RF cancellation for improved isolation in simultaneous transmit–receive systems," *IEEE Trans. Microw. Theory Techn.*, vol. 66, no. 5, pp. 2299–2312, May 2018.

[82] A. Elmaghraby *et al.*, "A mixed-signal technique for TX-induced modulated spur cancellation in LTE-CA receivers," *IEEE Trans. Circuits Syst. I, Reg. Papers*, vol. 65, no. 9, pp. 3060–3073, Sep. 2018.

[83] S. Sadjina, K. Dufrêne, R. S. Kanumalli, M. Huemer, and H. Pretl, "A mixed-signal circuit technique for cancellation of multiple modulated spurs in 4G/5G carrier-aggregation transceivers," in *IEEE Int. Solid-State Circuits Conf. (ISSCC) Dig. Tech. Papers*, Feb. 2019, pp. 356–358.

[84] E. Babakrpur and W. Namgoong, "Digital cancellation of harmonic and intermodulation distortion in wideband saw-less receivers," *IEEE Trans. Circuits Syst. II, Exp. Briefs*, vol. 65, no. 11, pp. 1554–1558, Nov. 2018.

[85] Z. Ru, N. A. Moseley, E. A. M. Klumperink, and B. Nauta, "Digitally enhanced software-defined radio receiver robust to out-of-band interference," *IEEE J. Solid-State Circuits*, vol. 44, no. 12, pp. 3359–3375, Dec. 2009.

[86] M. Ghadiri-Sadrabadi and J. C. Bardin, "A discrete-time RF signal-processing technique for blocker-tolerant receivers with wide instantaneous bandwidth," *IEEE Trans. Circuits Syst. I, Reg. Papers*, vol. 65, no. 12, pp. 4376–4389, Dec. 2018.

Silvester Sadjina (S'15) was born in Salzburg, Austria, in 1988. He received the B.Sc. and M.Sc. degrees in information electronics from Johannes Kepler University (JKU), Linz, Austria, in 2013 and 2015, respectively. He is currently pursuing the Dr.-Ing. (Ph.D.) degree at the Institute of Integrated Circuits, JKU, in cooperation with Danube Mobile Communications Engineering (DMCE) GmbH & Co KG (majority owned by Intel Austria GmbH), Linz.

In his studies, he specialized in measurement technology and communication engineering. In 2014, he was employed as a Research Assistant with the Institute for Measurement Technology, JKU. His research activities focus on the study and the development of mixed signal interference cancellation techniques for the mitigation of receiver performance degradation in cellular transceiver systems.

Christian Motz (S'17) was born in Vöcklabruck, Austria, in 1990. He received the bachelor's degree (Hons.) in hardware software design and the master's degree in embedded systems design from the School of Informatics, Communications and Media, University of Applied Sciences Upper Austria, Hagenberg, Austria, in 2013 and 2015, respectively. His master's thesis was focused on pattern matching cooperation with the Software Competence Center Hagenberg GmbH, Hagenberg. His thesis was on efficient implementation of Weyls discrepancy measure for 2-D image data. He is currently pursuing the Ph.D. degree at the Institute of Signal Processing, Johannes Kepler University (JKU), Linz, Austria, in cooperation with DMCE GmbH (Intel Linz), Linz.

From 2010 to 2015, he was with the University of Applied Sciences Upper Austria, Wels, Austria. In 2016, he joined the Research Center for Non Destructive Testing GmbH, Linz. Since 2017, he has been a member of the Institute of Signal Processing, JKU, and the CD Laboratory for Digitally Assisted RF Transceivers for Future Mobile Communications, where he is involved in receiver interference cancellation by means of adaptive signal processing methods.

Thomas Paireder (S'19) was born in Melk, Austria, in 1992. He received the bachelor's degree (Hons.) in information electronics and the master's degree (Hons.) in electronics and information technology from Johannes Kepler University (JKU), Linz, Austria, in 2016 and 2018, respectively. His master's thesis was focused on signal processing in cooperation with the Research Center for Nondestructive Testing GmbH. In his thesis, he implemented a real-time processing system for laser-ultrasonic signals. He is currently pursuing the Ph.D. degree at JKU in cooperation with DMCE GmbH (Intel Linz), Linz, with a focus on receiver interference cancellation by means of adaptive signal processing methods.

From 2012 to 2018, he was with JKU. Since 2018, he has been a member of the Institute of Signal Processing, JKU.

Mario Huemer (M'00–SM'07) was born in Wels, Austria, in 1970. He received the Dipl.-Ing. degree in mechatronics and the Dr.Techn. degree from Johannes Kepler University (JKU), Linz, Austria, in 1996 and 1999, respectively.

After holding positions in industry and academia, he became an Associate Professor with the University of Erlangen–Nuremberg, Erlangen and Nuremberg, Germany, from 2004 to 2007, and a Full Professor with Klagenfurt University, Klagenfurt, Austria, from 2007 to 2013. In September 2013, he moved back to Linz, where he is now heading the Institute of Signal Processing, JKU, as a Full Professor. Since 2017, he has been the Co-Head of the Christian Doppler Laboratory for Digitally Assisted RF Transceivers for Future Mobile Communications. His research focuses on statistical and adaptive signal processing, signal processing architectures, as well as mixed signal processing with applications in information and communications engineering, radio frequency transceivers for communications and radar, and sensor and biomedical signal processing.

Dr. Huemer is a member of the IEEE Signal Processing Society, the IEEE Circuits and Systems Society, the IEEE Communications Society, the IEEE Microwave Theory and Techniques Society, the German Society of Information Technology (ITG), and the Austrian Electrotechnical Association (OVE). He has received the dissertation awards of the German Society of Information Technology (ITG) and the Austrian Society of Information and Communications Technology (GIT), respectively, the Austrian Kardinal Innitzer Award in natural sciences, and the German ITG Award.

Harald Pretl (S'97–M'01–SM'08) received the Dipl.-Ing. degree in electrical engineering from the Graz University of Technology, Graz, Austria, in 1997, and the Dr.Techn. degree from Johannes Kepler University (JKU), Linz, Austria, in 2001.

He is currently a Sr. Principal Engineer with Intel Corporation, Linz, where he has been contributing to multiple generations of cellular RF transceivers and mobile communications platforms as an Analog Circuit Designer, a Project Lead, a Department Manager, and an RF Systems Architect. Since 2015, he has been a Full Professor with the Institute for Integrated Circuits (IIC), JKU, where he is heading the Energy-Efficient Analog Circuits and Systems Group. He has published more than 40 articles and presentations at international conferences and journals in the area of RF transceivers. He holds 25 issued and filed patents. His current research interests are focused on highly integrated GSM/UMTS/LTE/5G transceivers, integrated complementary metal–oxide–semiconductor (CMOS) PAs for mobile communications and IoT, wireless sensor networks, and low-power RF and mixed-signal SoC.

Dr. Pretl is a member of the IEEE Solid-State Circuits Society and the Austrian Electrotechnical Association (OVE). He was a member of the Technical Program Committee (TPC) of the International Solid-State Circuits Conference (ISSCC) in 2010–2012.